Evaluating multiple canopy-snow unloading parameterizations in SUMMA with time-lapse photography characterized by citizen scientists

Cassie Anne Lumbrazo

A thesis

Submitted in partial fulfillment of the

requirements for the degree of

Master of Science in Civil Engineering

University of Washington

2020

Committee:

Jessica Lundquist

Bart Nijssen

Program Authorized to Offer Degree:

Civil and Environmental Engineering

University of Washington

Abstract

Evaluating multiple canopy-snow unloading parameterizations in SUMMA with time-lapse photography characterized by citizen scientists

Cassie Anne Lumbrazo

Chair of the Supervisory Committee:

Professor Jessica Lundquist

Civil and Environmental Engineering

Snow in the canopy can sublimate back into the atmosphere, or unload to the surface and contribute to streamflow. Snow unloading results in a drastic, and sometimes sudden, decrease in the land surface albedo. Snow unloading is a complex physical process that is difficult to parameterize due to limited observations. Time-lapse photos of snow in the canopy were characterized by citizen scientists to create a dataset of snow interception observations at multiple locations across the western United States. This novel interception dataset was used to evaluate three snow unloading parameterizations in the Structure for Unifying Multiple Modeling Alternatives (SUMMA) modular modeling framework.

SUMMA was modified to include a third snow unloading parameterization (Roesch et al., 2001), which includes temperature and wind dependent unloading functions. This parameterization is compared to a meltwater drip unloading parameterization (Andreadis et al., 2009) and a time-dependent exponential unloading parameterization (Hedstrom & Pomeroy, 1998). The

parameterizations were calibrated at Niwot Ridge, CO, using hourly interception observations, and simulations with these calibrated parameters were compared to those using default (i.e., literature recommended) parameterizations at sites located at Niwot Ridge, CO, Grand Mesa, CO, and the maritime Olympic Mountains, WA. The Roesch et al., (2001) parameterization with temperature and wind unloading performed best at Niwot Ridge, where it captured 87% of the observed snow interception events. When parameterizations with wind dependent and exponential unloading were transferred to Grand Mesa and the Olympic Mountains, they unloaded snow from the canopy too rapidly. This suggested that parameterizations would need to be recalibrated for the unique interception physics of those domains. As a result, Andreadis et al., (2009), which retained snow in the canopy longest, captured the duration of snow in the canopy best when transferred to these additional sites. Unloading schemes also impacted the total sublimation modeled at each site. At Niwot Ridge, cumulative sublimation from the canopy was 87.6 mm using Andreadis et al., (2009) parameterization, which is 6% of the total winter precipitation, compared to Roesch et al., (2001), which sublimated 1% of the total precipitation. While canopy-snow unloading parameterizations are often overlooked in land surface models, results show that the unloading scheme can have an effect on the duration of snow in the canopy, impacting the land-surface albedo, and whether canopy-snow contributes to streamflow or sublimates.

1. Introduction.

Forest covers a significant portion of the Northern Hemisphere land surface and 40% of the North American snow zone (Klein et al., 1998). Depending on the climate, needleleaf coniferous forests can intercept 60-80% of total snowfall (Lundquist et al., 2013; Martin et al., 2013). The physical process of forest-snow interception has a large influence on the surface energy balance for these regions (Essery, 1998). Dense coniferous forests naturally have a low albedo. Once the evergreen canopy is covered with snow, the albedo of the entire land surface increases along with its energy feedback to the atmosphere. Although it is known that global climate models are particularly sensitive to the snow and ice albedo feedback, many still have poorly simulated land surface schemes that poorly simulate the winter albedo of a boreal forest (Bartlett & Verseghy, 2015; Bonan et al., 1992). Studies show that properly representing the physical processes involved in canopy interception can improve the simulated surface albedo over boreal forest regions (Niu & Yang, 2004).

To properly represent the albedo over forested areas, it is critically important to resolve the timing of snow unloading from the canopy once it is intercepted. Unloading results in a large, and sometimes sudden, decrease in land surface albedo. This complex physical process is difficult to parameterize due to limited observations, making existing model formulations difficult to evaluate. The goal of this work is to evaluate the performance of three widely used canopy snow unloading parameterizations, using a modular snow model that holds all other processes constant, combined with time-lapse photographs from three different locations in the Western U.S., interpreted by citizen scientists.

For comparison with default values, the three parameterizations are also calibrated at a continental site where reliable observed forcing data is available along with time-lapse photography of forest-snow interception. The three unloading parameterizations are calibrated using the observed meteorological data and then performance is evaluated with forcing data from an atmospheric model to determine how results change as a function of the type of atmospheric forcing data. Afterward, we use the atmospheric model's forcing data to test the unloading parameterizations in areas where we have interception observations interpreted by citizen scientists, but where we do not have temporally complete and quality controlled meteorological data. The calibrated model setup is then tested in other climates to evaluate local and regional scale model transferability of snow unloading parameterizations. All of the calibrated simulations are compared against simulations run with default parameter values to determine the parameterizations sensitivity to calibration, and transferability with calibrated vs. default parameter values.

This paper is arranged as follows. *Section 2* provides background on study sites and model forcing data, *Section 3* provides information about the novel interception dataset created by time-lapse photography used to evaluate model performance, outlines the three unloading parameterizations, explains model calibration, and the binary evaluation process used. *Section 4* describes the results of this study, and discussion about transferability and conclusions follow in *Sections 5* and *6*, respectively.

2. Study Sites and Forcing Data.

Snow unloading parameterizations were evaluated at four different locations: Niwot Ridge, CO where the model simulations were calibrated, two sites on Grand Mesa, CO where local scale model validation was done, and Mount Hopper, WA for regional scale model validation.

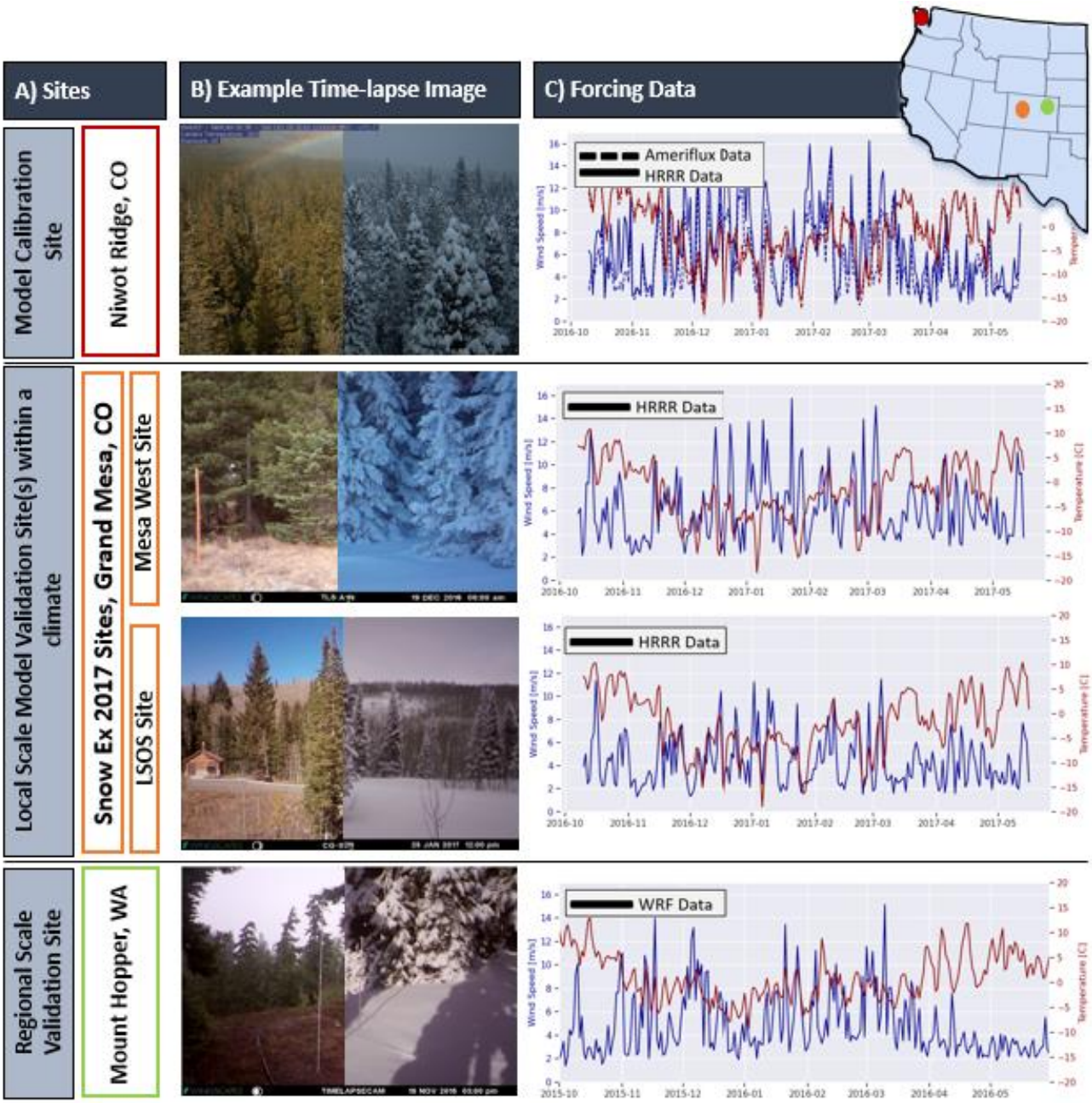

Figure 1. A). Study sites broken down into three classifications, the model calibration site is Niwot Ridge, CO, the local scale model validation sites are two sites on Grand Mesa, CO, and the regional scale validation site is Mount Hopper in Olympic National Park, WA. B). Example time-lapse images with and without snow for each site. C). Time-series of windspeed m s^{-1} (left y-axis in blue) and temperature ºC (right y-axis in red) from the Ameriflux, HRRR, and WRF forcing data used for each site.

2.1. Model Calibration Site: Niwot Ridge, CO

Niwot Ridge is located on the leeward side of the Continental Divide in Colorado, USA, and is a cold continental climate at 3050 m elevation. Niwot Ridge is a windy site with 7-8 m mixed Ponderosa Pine and Subalpine Fir. Time-lapse photos were taken every 30-minutes on the Ameriflux Tower, above the canopy, and were archived by the PhenoCam Network (Milliman et al., 2018). The classifications were aggregated to 1-hour interception observations during daylight hours.

Hourly forcing data for water year (WY) 2017 were collected from the onsite Ameriflux Meteorological Tower (Ameriflux Site US-NR1) at a 20 m measurement height. Since there is temporally complete observed meteorological data available, the unloading parameterizations were first calibrated at Niwot Ridge and compared to default parameter value simulations.

Additional simulations with default and calibrated unloading parameters were run using the High-Resolution Rapid Refresh (HRRR) atmospheric model (Horel & Blaylock, 2019) at 3-km spatial resolution. The goal of these additional model runs was to test how the unloading parameterizations change using a different forcing data source. At most sites, we only have atmospheric model output available and not high-quality flux tower in-situ data, such as Niwot Ridge. We compare the sensitivity of HRRR at Niwot Ridge, where we have reliable meteorological data and proceed with atmospheric model forcing data at sites with interception observations, but not quality controlled meteorological data. While this does not allow us to fully evaluate the unloading at the other sites (i.e., HRRR data is good at Niwot Ridge, but not at Grand Mesa), we presume we have a reasonable forcing dataset to move forward with at sites with interception observations.

Ameriflux data showed a mean winter temperature, between 1 November and 1 April, of -4.4 ºC and mean wind speed of 6.0 m s^{-1} reaching up to 21.5 m s^{-1}. HRRR data showed a mean winter temperature, between 1 November and 1 April, of -3.9 ºC and mean windspeed of 7.56 m s^{-1}, reaching up to 27.1 m s^{-1} (Table 1).

2.2. Local Scale Model Validation Sites: Grand Mesa, CO

Transferability of the default and calibrated unloading parameterizations was tested at two sites on Grand Mesa in Colorado, USA, where NASA's 2017 SnowEx Field Campaign took place. Grand Mesa was chosen to evaluate the transferability of the parameters within a region with similar mean winter temperature and wind speeds as Niwot Ridge. Additionally, Grand Mesa offered the ability to test the model's performance at two different locations with exposure to the same storms, but with different wind speeds.

The Mesa West (MW) site is located on the west end of the mesa at 3033 m, it is an exposed and windy location. HRRR data from WY 2017 shows a mean winter temperature, between 1 November and 1 April, of -4.5 ºC and a mean wind speed of 6.5 m s^{-1}, reaching up to 23.8 m s^{-1}. In contrast, the Local Scale Observational Site (LSOS) is located just off the mesa at 2974 m, with a mean winter temperature of -4.8 ºC and mean wind speed of 4.5 m s^{-1}, reaching up to 16.1 m s^{-1} for the same dataset and timeframe (Table 1). While there are meteorological stations available at each site, environmental conditions make them subject to riming, making wind speed data temporally inconsistent through the winter months. Thus, forcing data for both sites was

taken from HRRR for WY 2017. Time-lapse photos were taken 5 times per day, at both sites providing interception observations approximately every 2 hours during daylight hours.

2.3. Regional Scale Model Validation Site: Mount Hopper, Olympic Mountains, WA

Mount Hopper is a maritime site, located in Olympic National Park in Washington State, USA at an elevation of 1864 m. Mount Hopper was used to test the regional model transferability of the default and calibrated snow unloading parameterizations from a cold continental climate to a warmer maritime-snow climate. Interception observations are similar to the Grand Mesa sites, where time-lapse photos were taken every 3 hours, during daylight hours, as a part of the OLYMPEX ground validation campaign during WY 2016 (Currier et al., 2017).

The unloading parameterizations were tested using forcing data from the Weather Research and Forecasting (WRF) Model (Skamarock et al., 2008) at 4/3 km spatial resolution, provided by the Northwest Modeling Consortium (Mass et al., 2003), for WY 2016 because HRRR was not archived before WY 2017. These WRF data are at a higher spatial resolution than HRRR and were specifically evaluated during the OLYMPEX campaign (Currier et al., 2017). When these data were combined with SUMMA, they produced unbiased estimates of peak SWE and captured the timing and magnitude of snowfall events during the accumulation season (Currier et al., 2017). Both WRF and HRRR simulations used the Thompson et al., (2004, 2008) microphysical scheme without convective parameterizations. Incoming shortwave and longwave radiation used the Rapid Radiative Transfer Model (Mwlaler et al., 1997). WRF data from WY 2016, between 1 November and 1 April, showed a mean air temperature of -1.6 ºC and mean wind speed of 5.8 m s^{-1}, reaching up to 27.2 m s^{-1} at Mount Hopper (Table 1).

Table 1. Site water year (WY), data source, and forcing data means and totals calculated between 1 November and 1 April of the specified WY.

Site	WY	Source	Mean Temp ºC	Mean Wind m s^{-1}	Total Precip mm
Niwot Ridge, CO	2017	Ameriflux	-4.4	7.6	1520
Niwot Ridge, CO	2017	HRRR	-3.9	6.0	978.4
MW, Grand Mesa, CO	2017	HRRR	-4.5	6.5	1274
LSOS, Grand Mesa, CO	2017	HRRR	-4.8	4.5	1876
Mount Hopper, WA	2016	WRF	-1.6	5.8	2409

3. Methods.

3.1. Citizen Science Interception Observations.

Modeling snow interception and unloading is difficult due to complex forest-snow interactions and limitation of conducting experiments in a laboratory environment. Time-lapse photography is a unique tool that can capture forest-snow processes in remote areas and adverse weather conditions. Images from high-resolution digital cameras taking automatic time-lapse photos were

collected from the PhenoCam Network (Milliman et al., 2018), the 2017 NASA SnowEx Field Campaign (Currier et al., 2019), and the Olympic Mountain Experiment (OLYMPEX) ground validation campaign (Lundquist et al., 2018; Houze et al., 2017; Currier et al., 2017) and uploaded to a citizen science platform called Zooniverse (*Zooniverse.org*), as the project titled, Snow Spotter.

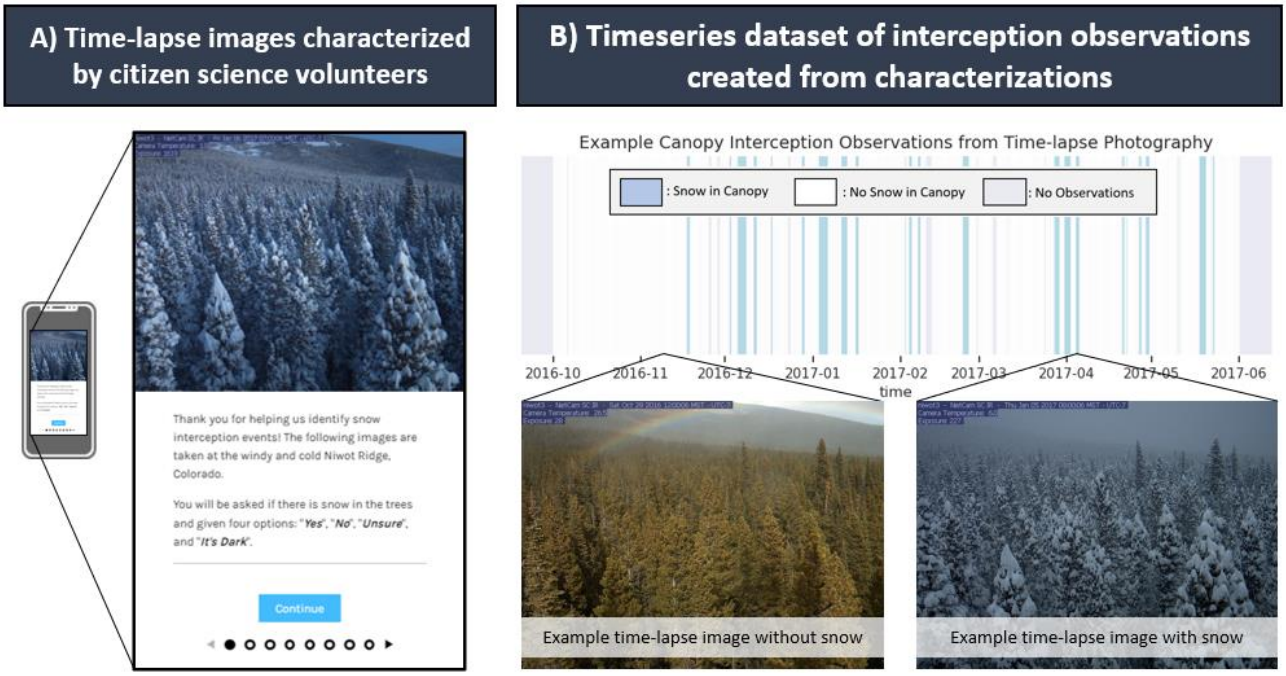

Figure 2. Time-lapse images were collected for each site and uploaded to the citizen science platform, Zooniverse, where A). online volunteers responded to a number of questions about snow in the canopy. B) An example of the processes data for one water year with example time-lapse images with and without snow in the canopy. The vertical lines represent the binary observations where blue is observations of snow in the canopy, white is no snow in the canopy, and gray is no observations.

The goal of Snow Spotter was to utilize citizen scientists to collect information about canopy interception. A total of 6,700 volunteer citizen scientists responded to a number of questions about 13,600 images from 13 sites across the United States. The question used in this research that provided the most quantitative information was, “Is there snow in the trees?” where citizen scientists could respond “Yes” or “No”. There were 9-15 classifications per image and volunteers agreed on the classification 95-98% of the time, depending on the site. The mean was taken for all classifications on a single image and if more than half of the volunteers agreed that there was snow in the trees, then it was recorded as snow present in the final dataset; otherwise it was recorded as no snow present. A binary time-series interception dataset was created from this data.

3.2. Modeling Snow Unloading Parameterizations in SUMMA

Three widely used canopy-snow unloading parameterizations were evaluated within the Structure for Unifying Multiple Modeling Alternatives (SUMMA) model (Clark et al., 2015a,b,c) using the time-lapse photography described in *Section 3.1*. SUMMA version 3 is the first release to contain Roesch et al., (2001) and thus, the first version to contain all three unloading parameterizations. SUMMA is a modular modeling framework and thus has the capability of evaluating each unloading parameterization independently, by holding all other processes constant.

The tree unloading parameterization available in SUMMA include 1) snow leaves the canopy through meltwater drip, which facilitates a specified percentage of snow in the canopy, relative to melt, that falls off in solid form (Andreadis et al., 2009); 2) snow unloads from the canopy using an exponential decay rate as a function of time after an interception event, independent of the other physical processes (Hedstrom & Pomeroy, 1998); 3) snow unloads as a function of both temperature and wind, each bound by minimum constraints (Roesch et al., 2001).

Snow unloading from the canopy, U, is only one piece of a system of equations which determines the snow water equivalent, (SWE), in the canopy at any specified timestep. SWE in the canopy, SWE_C, is defined as,

$$SWE_c = P - E - U, \quad \text{(Eq. 1)}$$

where *P* is precipitation as rain and snow and *E* is the latent heat flux in the canopy which includes evaporation and sublimation of liquid from the vegetation. Snow can unload from the canopy through two physical processes,

$$U = U_s + U_m \quad \text{(Eq. 2)}$$

where U_s represents solid snow unloading and sluffing off the canopy as a mass, contributing to the snowpack below the canopy, and U_m represents snow melting within the canopy and dripping off the vegetation, onto the snowpack below.

In this work, only parameterizations directly impacting U are evaluated, while rates impacting all other physical processes are held constant. Although rates and parameters controlling other processes as held constant, such as parameters controlling the latent heat flux, changes in U impact the overall SWE_C and thus, values for the evaporation, transpiration, and sublimation from the vegetation in the canopy can vary between simulations of each unloading parameterization when the amount of snow in the canopy changes. For the specific SUMMA model setup, model decisions and parameter names used in this paper, see Appendixes A and B, respectively.

3.2.1. Meltwater Drip Unloading (Andreadis et al., 2009)

The first unloading parameterization evaluated is formulated in Andreadis et al., (2009) and represents snow unloading from the canopy, U_s, as

$$U_s = 0, \qquad for\ L_c \leq L_m, \quad \text{(Eq. 3)}$$

$$U_s = p \cdot U_m, \quad for\ L_c > L_m, \quad \text{(Eq. 4)}$$

where L_C is liquid water accumulating on the vegetation canopy at a given time, kg m^{-2} s^{-1} and L_m is the maximum liquid water storage available before canopy drainage begins, kg m^{-2} s^{-1}. U_m is the canopy liquid drainage flux of liquid water from the vegetation canopy, kg m^{-2} s^{-1}, and p is the percent of solid snow that unloads from the canopy to the snowpack below once the liquid water storage in the canopy has been exceeded. Storck et al., (2002) observed unloading when air temperatures were above 0ºC in Umpqua, Oregon and determined that approximately 40% of the canopy snow is unloaded coincident with melting. This percent, *p*, is a tunable parameter in SUMMA with a default value of 0.4, but it can be set anywhere in the range of 0-1 (Appendix A).

3.2.2. Exponential Unloading (Hedstrom & Pomeroy, 1998)

The second unloading parameterization evaluated uses an exponential decay function to unload a mass of snow form the canopy as a function of time, *t*, to the snow beneath the canopy. This parameterization, formulated in Hedstrom & Pomeroy, (1998), defines the mass of snow unloading from the canopy, U, as

$$U_s = I_s(e^{-kt}), \quad \text{(Eq. 5)}$$

where I_s is the intercepted snow in the canopy at a given timestep, kg m^{-2} s^{-1}, and k is the exponential coefficient of unloading as a function of time, s^{-1}. In this parameterization, there is only solid snow unloading from the canopy, U_s, and no physical melt happening within the vegetation. Observations from Hedstrom & Pomeroy, (1998) suggest a coefficient of unloading value of $k = 0.0006467$ s^{-1}, and this value is a tunable parameter in SUMMA (Appendix A).

3.2.3. Temperature and Wind Dependent Unloading (Roesch et al., 2001)

The third unloading parameterization evaluated is formulated in Roesch et al., (2001), who wanted a better way to represent the albedo over forests, and created a snow unloading schemes which includes temperature and wind dependent unloading functions. The snow unloading from the canopy, U_s, defined as,

$$U_s = I_s[f(T_c) + f(v)], \quad \text{(Eq. 6)}$$

where $f(T_c)$ is the temperature dependent unloading function and T_c is the canopy air temperature. $f(v)$ is the wind dependent unloading function and v is the wind speed at the top of the canopy. $f(T_c)$ is defined as

$$f(Tc) = \frac{Tc - T_m}{C_t}, \quad \text{(Eq. 7)}$$

where T_m is the minimum temperature that snow can start unloading. This value is suggested as $T_m = 270.15\ K$ (-3 ºC) and is a tunable parameter value in SUMMA (Appendix A). C_t is the rate at which snow unloads from the canopy after the minimum temperature is met. This value is suggested as $C_T = 1.87x10^5\ s^{-1}$and is a tunable parameter value in SUMMA (Appendix B).

The wind dependent unloading function, $f(v)$, is defined as

$$f(v) = 0, \qquad for\ v\ < v_m \tag{Eq. 8}$$

$$f(v) = \frac{v}{C_v}, \qquad for\ v\ \geq v_m \tag{Eq. 9}$$

where C_v is the rate a which wind is unloading snow from the canopy, s^{-1}, and v_m is the minimum wind speed required for wind dependent unloading to occur. Thus, once the wind speed at the top of the canopy is equal to the minimum wind speed, intercepted snow unloads from the canopy at the specified rate, C_v. Both the rate of wind unloading and the minimum wind speed for unloading are tunable parameter values in SUMMA (Appendix B). In this unloading parameterization, there is only solid snow unloading from the canopy, U_s, even within the temperature unloading function, snow does not melt within the canopy. Instead once the temperature constraints are satisfied, snow will unload at the rate, C_T, and contribute to the snowpack below the canopy.

3.3. Model Evaluation Metrics.

As described in *Section 3.1.*, the canopy interception dataset consists of a binary time-series of no snow and snow in the canopy. However, the model simulations from SUMMA are a continuous timeseries of SWE in the canopy in millimeters for each timestep. To evaluate the model performance, the model simulation was reduced to a binary dataset. First, a minimum snow threshold is set at 2 mm of SWE, suggesting that any snow accumulation under 2 mm of SWE is not enough accumulation to be a hydrologically significant interception event (Schmidt & Gluns, 1991). Thus, for any timestep with snow in the canopy greater than 2 mm, the model is reduced to binary information such as snow is present in the canopy, while every other timestep becomes no snow present in the canopy.

		Observations of Unloading	
		Snow	No Snow
Modeling Unloading	Snow	**True Positive (TP)** Model Snow, Obs snow	**False Positive (FP)** Model Snow, Obs no snow
	No Snow	**False Negative (FN)** Model no snow, Obs snow	**True Negative (TN)** Model no snow, Obs no snow

Figure 3. A confusion matrix used to describe the performance of the binary unloading model to the binary interception observations.

The binary time-series are evaluated together to determine the following metrics: True Positive (TP),when the model and the observations have snow in the canopy, False Positive (FP), when the model has snow in the canopy but the observations do not, True Negative (TN), when the model and the observations do not have snow in the canopy, and False Negative (FN), when the model does not have snow in the canopy, but the observations do.

The binary evaluation metric, Balanced Accuracy (BA), is used in this work as a measure of model performance. The BA score is the average accuracy obtained for either class (Brodersen et al., 2010), defined as,

$$Balanced\ Accuracy\ (BA)\ = \frac{1}{2}\left(\frac{TP}{TP+FN} + \frac{TN}{TN+FP}\right). \quad \text{(Eq. 10)}$$

Unlike the commonly used F-score, the BA score is symmetric in its weight for both TP and TN results; thus, it will capture when the model performs accurately in both the presence and absence of snow in the canopy. The F-score is another metric used to evaluate binary data, which excludes TN values (Olson & Delen, 2008). This has often been used to evaluate snow covered area products since the absence of TN values prevents unfairly weighing summer periods of no snow. We only evaluated interception during the winter months; thus, all components of the confusion matrix are important when evaluating model performance in this work (Table 3).

3.4. Model Calibration.

The three canopy snow unloading parameterizations were evaluated independently in SUMMA by holding all other processes constant. Model evaluation started at Niwot Ridge, which has reliable observed meteorological forcing data and a high likelihood for wind unloading events (i.e., one of the physical unloading processes being tested), using hourly interception observations. All three unloading parameterizations were calibrated using the observed meteorological data. The model set up was evaluated with forcing data from an atmospheric model (i.e., HRRR) at Niwot Ridge, to assess the impact of changing the forcing data source on the model's performance. These calibrated model simulations were compared against default model runs.

Complex model parameter interactions make isolating only unloading processes difficult. The overall accumulation of snow in the canopy impacts the timing of unloading (i.e., the larger the snow load, the longer it takes to unload at a fixed rate). To limit the degrees of freedom, parameters impacting snow accumulation (i.e., canopy interception) were held constant between all the calibration runs, such as the specified interception parameterizations impacting accumulation and the parameter which controls the maximum amount of intercepted snow that can be retained by the canopy.

Calibration analysis showed that the parameter impacting unloading in the Andreadis et al. (2009) parameterization, p, the percent of solid snow that unloads from the once the liquid water storage in the canopy has been exceeded, was not sensitive at Niwot Ridge. Since Niwot Ridge is a cold site, the canopy-snow did not melt mid-winter, and the BA did not change when tested in the full parameter range 0-1. Thus, analysis proceeded with the suggested value in the literature for this parameter, which is 0.4 (Storck et al., 2002). The value of 0.4 is also used in the default model simulations.

The Hedstrom and Pomeroy, (1998) exponential decay unloading parameterization has a single parameter sensitive to unloading, which is k, the exponential coefficient of unloading. k was tested within the full suggested parameter range and the parameter value with the highest BA score was selected (Appendix, Table 1). For the default model runs, the suggested unloading coefficient was used (Appendix, Table 1).

Roesch et al. (2001) includes two primary unloading functions, wind and temperature, which each have two tunable parameters in SUMMA. There are complex parameter/parameter interactions within this unloading scheme (i.e., adjusted minimum wind threshold and rate of wind unloading). To limit the interactions of the two parameter values within the wind unloading function, v_m, the minimum wind speed required for wind dependent unloading was held constant at 5 m s^{-1}(Betts & Ball, 1997; Miller, 1962; Roesch et al., 2001). The temperature dependent unloading function was not sensitive at Niwot Ridge since it is a cold site. Thus both tunable temperature dependent parameter values were held constant; T_m , the minimum temperature for snow unloading, was held constant at the suggested parameter value of $T_m = 270.15\ K$ (-3 ºC) and the rate of temperature dependent unloading, C_T, was held constant at the suggest value of $C_T = 1.87x10^5$ s^{-1}. These suggest parameter values are also used in the default model simulations. The only parameter calibrated for this unloading parameterization was, C_v, the minimum wind speed required for wind dependent unloading. Reducing this parameterization to one free parameter provides opportunity for comparison across the three unloading parameterization since calibration resulted in the same degrees of freedom for each unloading scheme. C_v was tested in the full parameter range and the value with the highest BA score was selected and the default parameter value equal to the suggested rate in the literature (Appendix, Table 1).

Both Andreadis et al. (2009) and the temperature dependent unloading function in Roesch et al. (2001) were not calibrated for Niwot Ridge. It is common practice to calibrate interception schemes to a single site with reliable meteorological data and since Niwot Ridge was not sensitive to the parameters within those two parameterizations, the parameter values were taken from the literature. The literature value used for the parameter in Andreadis et al. (2009) was calibrated by Storck et al. (2002) in Umpqua, Oregon. Umpqua is a maritime climate similar to, and not far from our Mount Hopper site in Olympic National Park, WA. Transferability of the unloading parameterizations was tested after calibration by running simulations with this parameter set at Grand Mesa and Mount Hopper. See Appendix Table 1 for SUMMA model parameter values and details. The calibrated model runs are compared to default model simulations at all sites (Table 2).

4. Results.

Three calibrated and independent unloading parameterizations were evaluated at Niwot Ridge, with observed meteorological data from the Ameriflux station and HRRR data. The model simulations were transferred to MW and LSOS at Grand Mesa, CO and at Mount Hopper, WA (Figure 4).

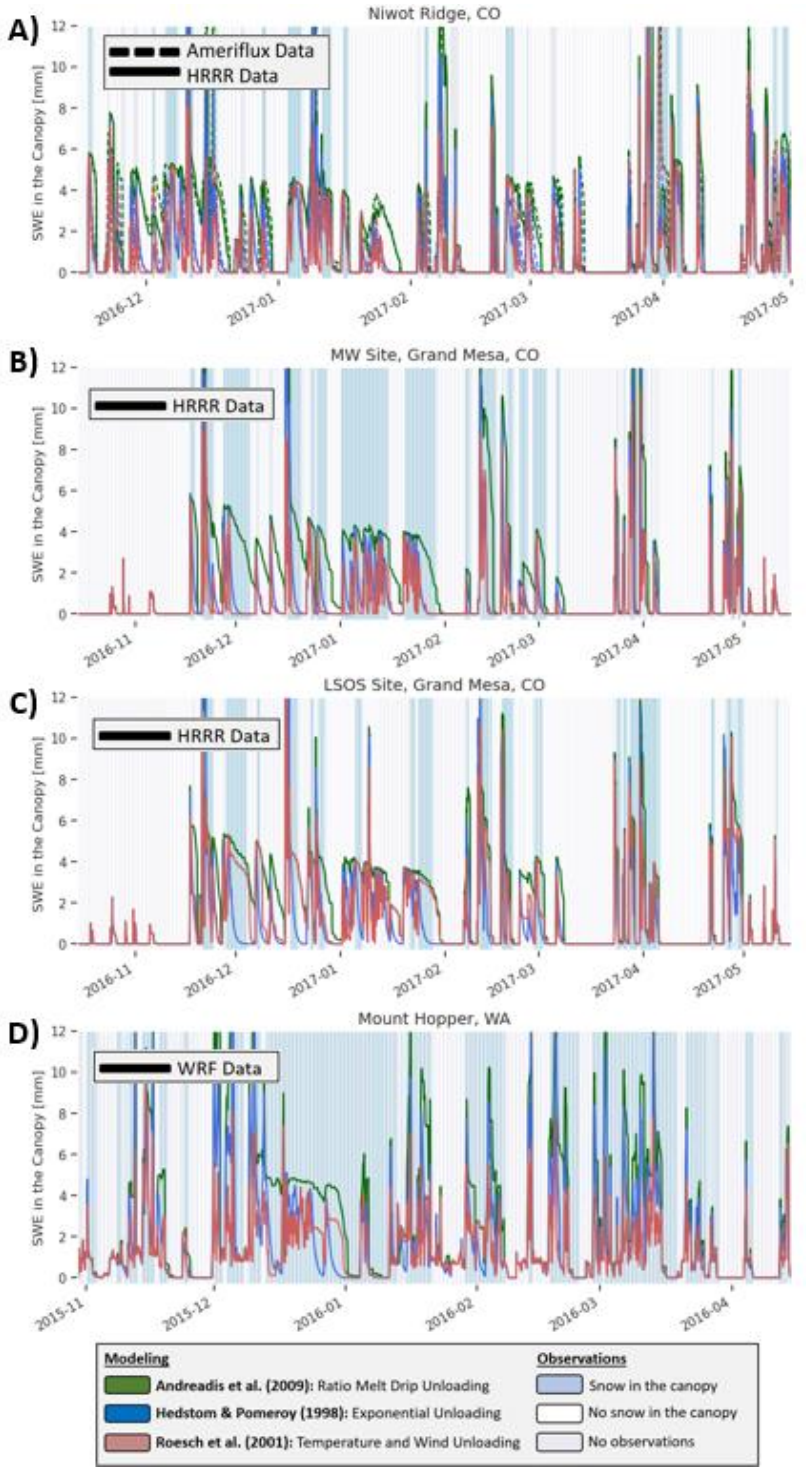

Figure 4. SUMMA model simulations showing all three unloading parameterizations for, A) Niwot Ridge, Colorado with Ameriflux (dashed line) and HRRR (solid line) forcing data, B) MW and C) LSOS sites on Grand Mesa, Colorado, and D) Mount Hopper in Washington. Binary interception observations are represented by the vertical lines where blue is observations of snow in the canopy, white is no snow in the canopy, and grey is no observations.

4.1. Model Calibration Site: Niwot Ridge, CO

For the default model runs at Niwot Ridge, CO, for WY2017, the Andreadis et al., (2009) unloading parameterization had a BA score of 0.78, Hedstrom & Pomeroy, (1998) of 0.74, and Roesch et al., (2001) of 0.82 when forced with the in situ Ameriflux data (Table 2). After model calibration, Hedstrom & Pomeroy, (1998) had a BA score of 0.80, and Roesch et al., (2001) of 0.85 when forced with the in situ Ameriflux data (Table 2).

Default model simulations with the HRRR atmospheric model forcing data resulted in a BA score of 0.78 for Andreadis et al., (2009) and 0.87 for Roesch et al., (2001). However, the default BA score was 0.63 for Hedstrom & Pomeroy, (1998) before calibration (Table 2). After calibration, Hedstrom & Pomeroy, (1998) had a BA score of 0.82, and Roesch et al., (2001) of 0.87 (Table 2).

For both sets of forcing data, Hedstrom & Pomeroy, (1998) had the largest BA score improvement between the default and calibration model simulations, improving 19% after calibration with HRRR forcing data. Andreadis et al., (2009) did not change, since the same parameter values were used in both runs and Roesch et al., (2001) improved slightly with calibration. There was not any large differences or sensitivities when switching between forcing data, suggesting that HRRR was as effective as in situ data meteorological forcing for Niwot Ridge.

The Roesch et al., (2001) unloading parameterization, which includes wind dependent unloading, had the highest BA score at Niwot Ridge for both forcing datasets by correctly simulating canopy snow presence at 87% of the hourly observational timesteps when calibrated. Roesch et al., (2001) correctly simulated canopy snow presence at 5% more timesteps than Hedstrom and Pomeroy, (1998), the exponential unloading scheme, and at 10% more timesteps correctly than Andreadis et al., (2009), which experienced a loss from canopy sublimation but only unloaded snow from the canopy when temperatures exceeded 0ºC.

4.2. Local Scale Model Validation Sites: Grand Mesa, CO, MW and LSOS

The default model simulations at the MW Site in Grand Mesa, CO for WY 2017 resulted in Andreadis et al., (2009) with a BA score of 0.83, Hedstrom & Pomeroy, (1998) of 0.58, and Roesch et al., (2001) of 0.78 (Table 2). Before calibration, Andreadis et al., (2009) simulated 83% of timesteps (i.e., every 2 hours) correctly, 25% more than Hedstrom & Pomeroy, (1998) and 5% more than Roesch et al., (2001). However, after calibration, Hedstrom & Pomeroy, (1998) had a BA score of 0.83, and Roesch et al. (2001) of 0.74 (Table 2). Thus, after calibration Hedstrom & Pomeroy, (1998) improved 25% and matches Andreadis et al., (2009) at simulating 83% of the timesteps correctly.

The default model simulations at the LSOS Site in Grand Mesa, CO for WY 2017 resulted in Andreadis et al., (2009) with a BA score of 0.79, Hedstrom & Pomeroy, (1998) of 0.57, and Roesch et al., (2001) of 0.78 (Table 2). Before calibration, Andreadis et al., (2009) simulated 79% of timesteps (i.e., every 2 hours) correctly, 22% more than Hedstrom & Pomeroy, (1998). Before calibration, Roesch et al., (2001) performed similarly to Andreadis et al., (2009).

However, after calibration, Hedstrom & Pomeroy, (1998) had a BA score of 0.79, and Roesch et al. (2001) also of 0.79 (Table 2). Thus, after calibration all three unloading schemes performed the exact same, simulating 79% of the canopy interception timesteps correctly.

4.3. Regional Scale Validation Site: Mount Hopper, WA

The default model simulations at Mount Hopper, WA for WY 2016 resulted in Andreadis et al. (2009) with a BA score of 0.78, Hedstrom & Pomeroy, (1998) of 0.51, and Roesch et al. (2001) of 0.70 (Table 2). Before calibration, Andreadis et al., (2009) simulated 78% of timesteps (i.e., every 3 hours) correctly, 27% more than Hedstrom & Pomeroy, (1998). After calibration, Hedstrom & Pomeroy, (1998) had a BA score of 0.68, yielding a 17% improvement, and Roesch et al., (2001) slightly decreased in performance after calibration with a BA score of 0.67. While this decrease is small (i.e., 3%), it suggests that calibrating the wind unloading function at a windy site, such as Niwot Ridge, and transferring it to Mount Hopper, WA actually decreases the model's performance. Andreadis et al., (2009) performed 10% better than both other unloading schemes at Mount Hopper after calibration.

Table 2. Model Simulation Results with BA scores for all three unloading parameterizations using the default parameter values and the parameter values calibrated at Niwot Ridge, CO and transferred to the other sites.

Balance Accuracy (BA) Scores for All Unloading Parameterizations			
Unloading Parameterizations Sites	**Andreadis et al., (2009)**	**Hedstrom & Pomeroy, (1998)**	**Roesch et al., (2001)**
Default Values			
Niwot Ridge, CO with Ameriflux	0.78	0.74	0.82
Niwot Ridge, CO with HRRR	0.78	0.63	0.84
MW, Grand Mesa, CO	0.83	0.58	0.78
LSOS, Grand Mesa, CO	0.79	0.57	0.78
Mount Hopper, WA	0.78	0.51	0.70
Calibrated at Niwot Ridge, CO and transferred to other sites			
Niwot Ridge, CO with Ameriflux	0.78	0.80	0.85
Niwot Ridge, CO with HRRR	0.78	0.82	0.87
MW, Grand Mesa, CO	0.83	0.83	0.74
LSOS, Grand Mesa, CO	0.79	0.79	0.79
Mount Hopper, WA	0.78	0.68	0.67

4.3. Unloading event case studies.

Interception events occur on a small (i.e., hourly) scale, thus observing model performance over a full season (Figure 4) becomes difficult to dissect and analyze. To better evaluate what is physically happening between the unloading parameterizations, two specific case studies are outlined at Niwot Ridge for WY 2017; First, a simulated interception event with observations of

snow accumulation in the canopy while wind speeds were low (Figure5), and second, a simulated interception event which occurred during a storm when no snow accumulated in the canopy (Figure 6).

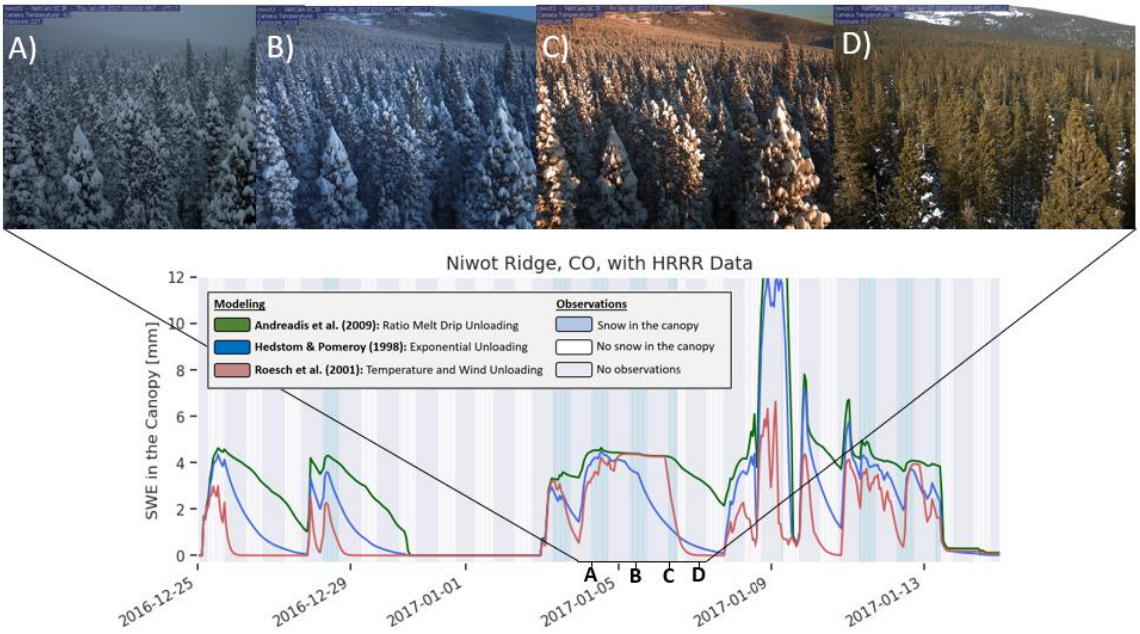

Figure 5. Unloading Event Case Study 1: An interception event calibrated at Niwot Ridge, CO between 2 and 7 January, 2017 when a large amount of snow accumulated in the canopy, shown in images A, B, and C, then snow unloaded from the canopy, shown in image D, a few hours later. Binary interception observations are represented by the vertical lines where blue is observations of snow in the canopy, white is no snow in the canopy, and grey is no observations.

The first case study highlights an interception event when the mean wind speed during the storm was low (2.4 m s^{-1}) and observations showed a large accumulation of snow in the canopy (Figure 5). All three parameterizations, calibrated at Niwot Ridge, intercepted, and retained snow for the duration of the event, however, they varied in when the snow was unloaded from the canopy. The Andreadis et al., (2009) parameterization retains snow in the canopy longer than both Roesch et al. (2001) and Hedstrom & Pomeroy (1998), which unload snow on time with the observations. However, Roesch et al. (2001) and Hedstrom & Pomeroy, (1998) both unload snow, but for different reasons. Roesch et al., (2001) captured this unloading event by modeling the physical processes contributing to snow leaving the canopy (i.e., increased wind speed), while the exponential decay function in Hedstrom & Pomeroy, (1998) provided a good estimate of the unloading event without those physics. However, when this calibrated event is compared to the same event in default model simulations, then Hedstrom & Pomeroy, (1998) no longer provides a good estimate for the unloading event. Roesch et al., (2001), default or calibrated, captures the event similarly due to the physics in the parameterization.

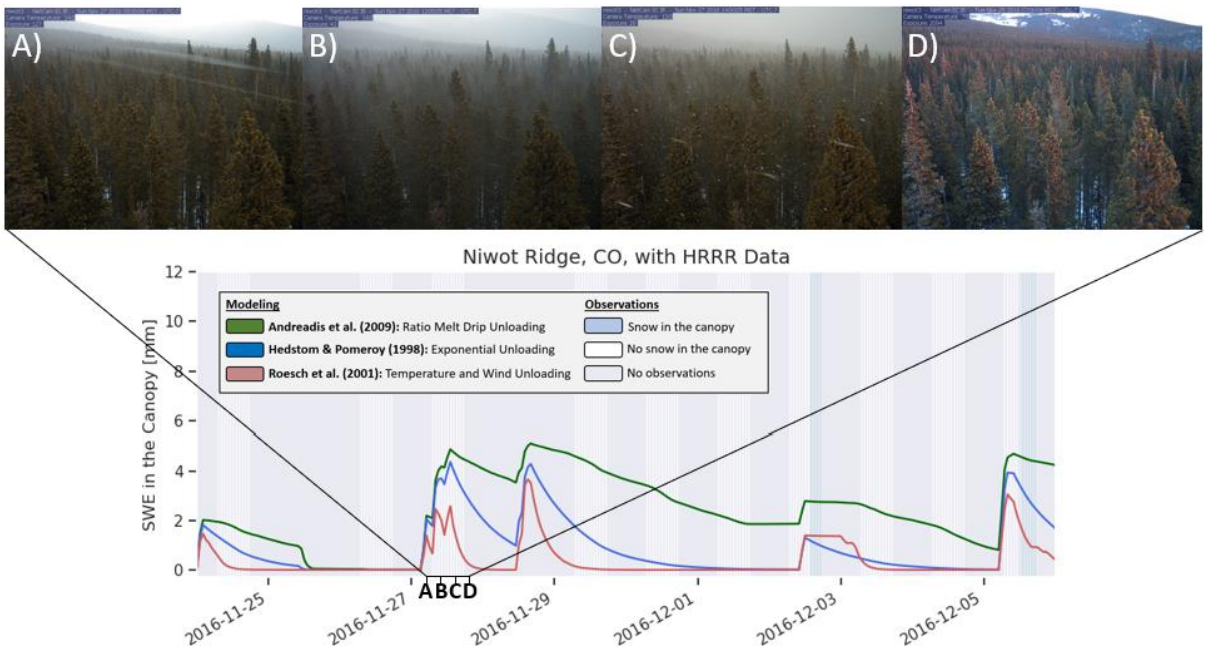

Figure 6. Unloading Event Case Study 2: A calibrated interception event at Niwot Ridge, CO between 27 and 29 November, 2016 when calibrated simulations model snow in the canopy during precipitation, but observations do not agree (shown in A, B, and C). After the storm passed, image D shows no snow accumulated in the canopy; however there is snow on the group beneath the canopy. Binary interception observations are represented by the vertical lines where blue is observations of snow in the canopy, white is no snow in the canopy, and grey is no observations.

The second case study highlights a modeled interception event, by all three parameterizations, when all observations show no snow in the canopy (Figure 6, A, B, C, D). Time-lapse images show a precipitation event occurring at a time with high winds, ending with no snow accumulating in the canopy and instead, only accumulating on the ground below the canopy. In this case, the exponential unloading in Hedstrom and Pomeroy, (1998) did not provide a good estimate for unloading in contrast to the physically-based Roesch et al., (2001) parameterization which completely unloaded snow in the canopy after a few hours. However, it is important to note that all three simulations accumulated snow in the canopy at this time step, even though the observations show no snow accumulating in the canopy. While this is not directly related to unloading parameterizations, the effectiveness of the interception scheme is going to impact the amount of snow in the canopy and when snow is in the canopy, and therefore, impact when and how much snow will unload.

5. Discussion.

5.1. Impact of fine-scale interception observations on model evaluation.

The interception observations used to calibrate this model were time-lapse photos taken every 30 minutes, with the exception of a few longer time periods of missing data. The classifications were aggregated to 1-hour interception observations during daylight hours. However, the model simulations were transferred to sites with interception observations available every 2 (i.e., Grand

Mesa) and 3 (i.e., Mount Hopper) hours. To determine if the calibrated model BA results were sensitive to the resolution of interception observations, the hourly observations from Niwot Ridge were resampled, hourly, between 1 hour and 24-hour interception observations (e.g., a 12-hour resample is 2 image per day) (Table 3).

Table 3. The BA scores for resampled interception observations at Niwot Ridge with HRRR forcing data.

Resampling Interception Observations at Niwot Ridge with HRRR Data			
Resample Observations	Andreadis et al., (2009)	Hedstrom & Pomeroy, (1998)	Roesch et al., (2001)
1 hour observations, 24 images/day	0.78	0.82	0.87
2 hour observations, 12 images/day	0.78	0.82	0.87
3 hour observations, 8 images/day	0.78	0.82	0.87
4 hour observations, 6 images/day	0.77	0.82	0.86
12 hour observations, 2 images/day	0.76	0.81	0.86
24 hour observations, 1 image/day	0.79	0.83	0.89

Resampling showed that the model evaluation metric used, BA, is not sensitive to the resolution of the interception observations (Table 3). This suggests that model performance should not be impacted by comparing the model simulations with observational datasets with different resolutions. However, it is important to note that interception observations created from time-lapse photography are limited to observations during daylight hours. All unloading model simulations were calibrated to observations taking place only during the daytime (e.g., only including daytime temperature ranges and wind patterns). This could bias the unloading parameterizations to only capture physical interception and unloading processes that occur during the day. However, the albedo in the canopy only matters during the day, thus the day-biased analysis is appropriate for this application.

5.2. Relationship between canopy-snow unloading, latent heat flux, and SWE beneath the canopy

Snow and meltwater in the canopy that were lost directly from the unloading parameterizations were defined as, *U*, canopy snow unloading, including both solid and liquid forms (Eq 2; Figure 7, B). In addition to unloading, *U*, snow in the canopy can be lost through latent heat flux, *E*, in the canopy (Eq. 1). *E* includes evaporation of liquid water and sublimation of snow from the canopy into the atmosphere. Case study 1, a low wind interception event from *Section 5.1.*, was evaluated for the canopy snow unloading (i.e., direct loss from unloading parameterizations) and loss from canopy sublimation (Figure 7).

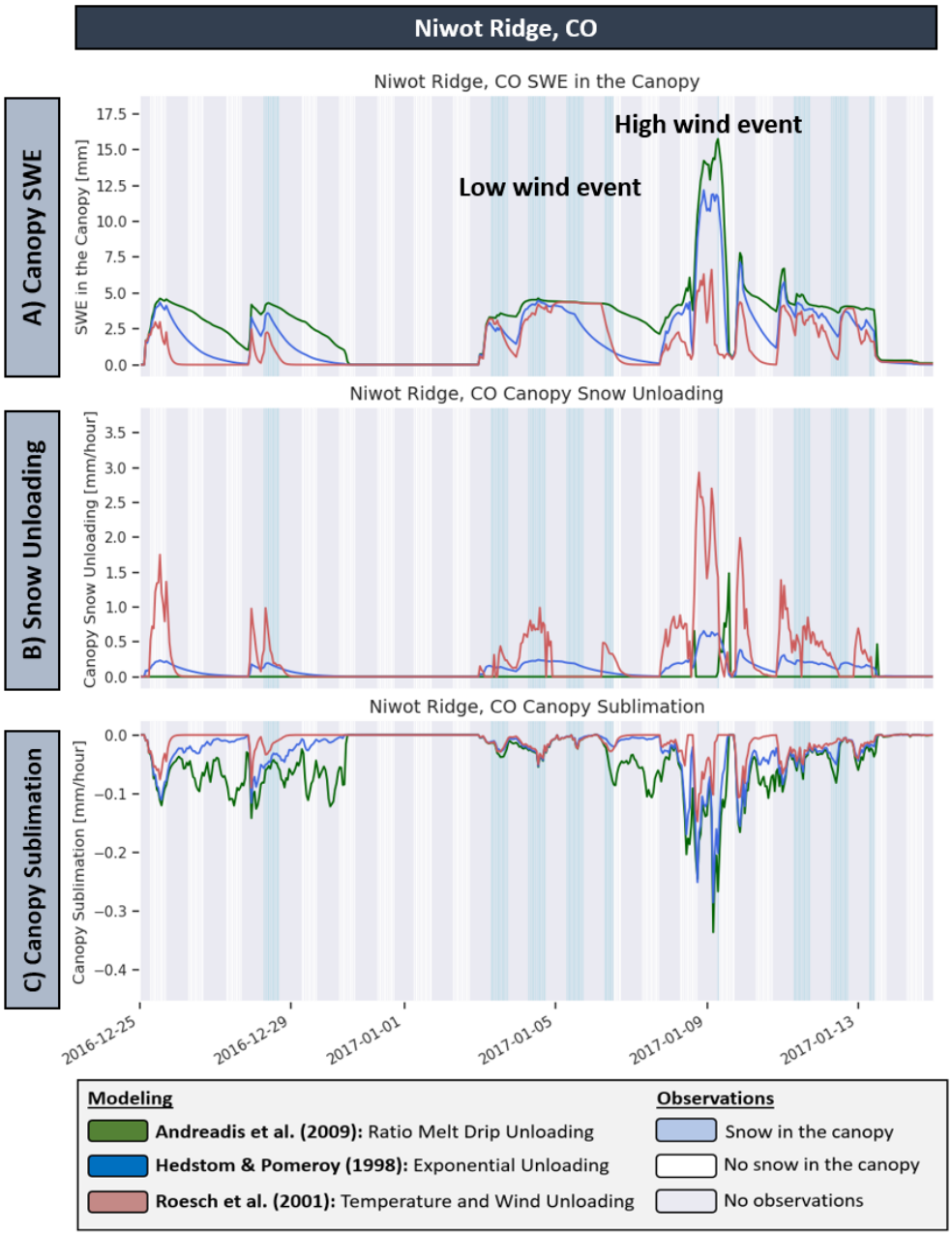

Figure 7. A) Canopy SWE mm, B) Snow unloading from the canopy, representing only the snow unloading from the canopy to the underlying snowpack, and C) Canopy sublimation, represented as a net loss from the hydrologic system (i.e., negative mm/hour of SWE) for Niwot Ridge, CO between 25 December, 2016 and 15 January, 2017, highlighting a low wind event when snow remained in the trees and a high wind event when observations did not show snow in the canopy. Binary interception observations are represented by the vertical lines where blue is observations of snow in the canopy, white is no snow in the canopy, and grey is no observations.

For this case study at Niwot Ridge, Roesch et al., (2001) has the highest amount of snow unloading from the canopy Figure 6B). Unloading from Roesch et al., (2001) increases with

increasing windspeed, but since snow was unloaded there, there was less snow left to sublimate. For this case study, Andreadis et al., (2009) unloads the least as a direct result of the unloading parameterization (Figure 6B). Since less snow unloaded during this event using the Andreadis et al. (2009) parameterization, Andreadis et al., (2009) led to move sublimation from the canopy (Figure 6C).

In addition to the instantaneous sublimation and unloading for case study 1 at Niwot Ridge, the cumulative sublimation, unloading, and SWE in the open vs. under the canopy were calculated for Niwot Ridge, CO for WY 2017 and Mount Hopper, WA for WY 2016.

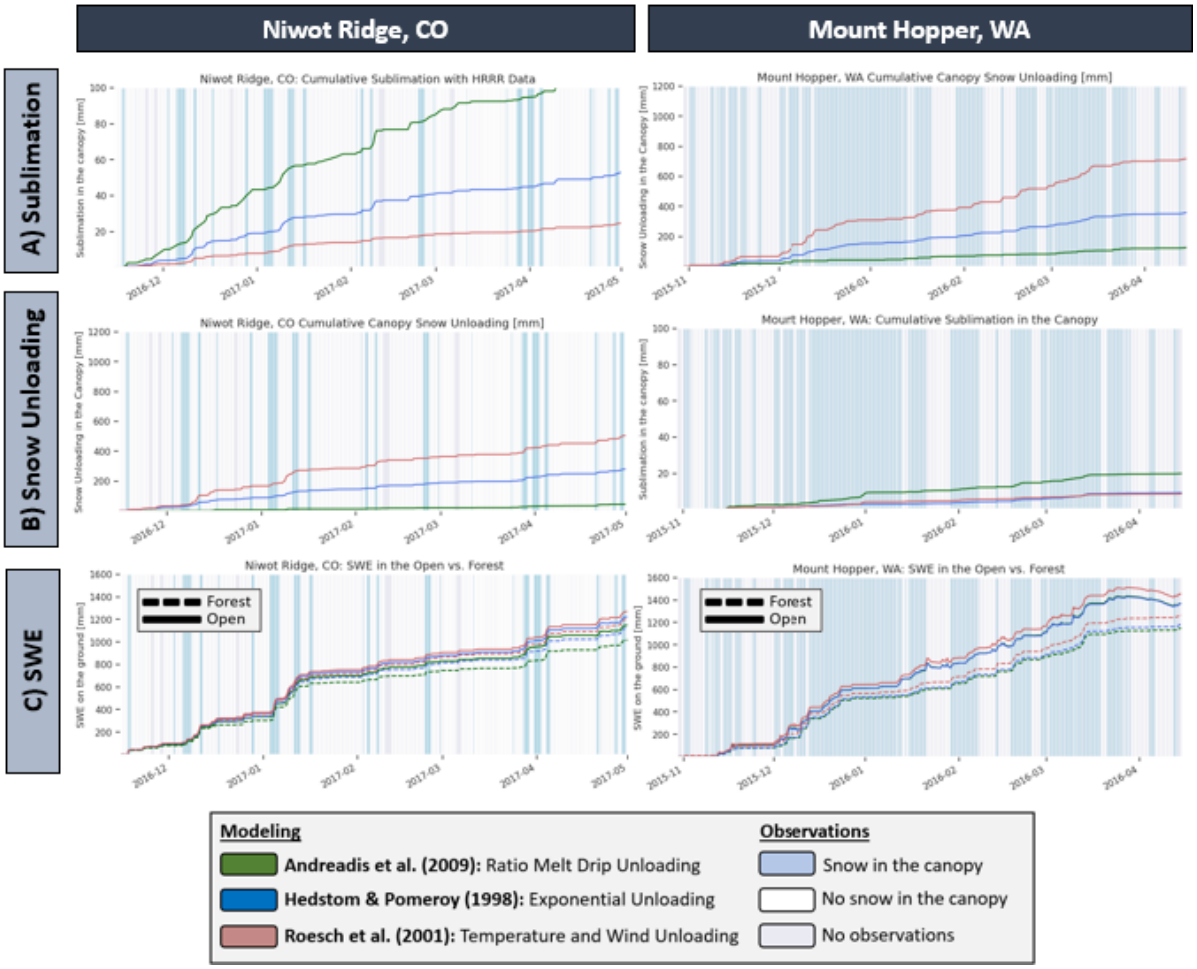

Figure 8. A) Cumulative sublimation of SWE (mm) in the canopy, B) Cumulative snow unloading from the canopy, and C) Cumulative SWE on the ground in the open (solid line) and the forest (dashed line), for Niwot Ridge, CO during HRRR data and Mount Hopper, WA. Binary interception observations are represented by the vertical lines where blue is observations of snow in the canopy, white is no snow in the canopy, and grey is no observations.

At Niwot Ridge, the model simulated a large loss through sublimation, specifically using Andreadis et al., (2009), which had a cumulative loss of 87.6 mm of SWE in the canopy and a total loss through sublimation as a percent of the total precipitation of 5.8 % (Table 3; Figure 8, A). The smallest cumulative sublimation was with the Roesch et al., (2001) which had a

cumulative loss of 25.2 mm of SWE in the canopy, equating to only 1.7 % of the total precipitation (Table 3; Figure 8, A). Roesch et al., (2001) has the largest cumulative snow unloading at both Niwot Ridge (510 mm) and Mount Hopper (721 mm) (Table 4). The loss of SWE in the canopy at Mount Hopper was driven by canopy snow unloading calculated in the parameterizations, since there was little total sublimation for all unloading parameterizations at Mount Hopper. In addition, these results impact the snowpack accumulation under the canopy (Figure 8C).

Unloading from the canopy to the land surface versus sublimation and evaporation is significant when the hydrologic model is coupled to an atmospheric model or the hydrologic model is used independently. For instance, during high wind events such as case study 1, the canopy unloading parameterization will determine the amount of snow that is unloaded to the surface where it will melt and contribute to runoff, vs. lost from the watershed through sublimation and returned back to the atmosphere as water vapor.

Table 3. The cumulative sublimation of SWE in the canopy [mm] and the total sublimation as a percent of the total precipitation [%] for each unloading parameterization.

Cumulative Sublimation of SWE in the Canopy [mm] and Total Sublimation as a percent of Total Precipitation [%]						
Unloading Scheme	Andreadis et al., (2009)		Hedstrom & Pomeroy, (1998)		Roesch et al., (2001)	
Calculation Site	Total Sublimation [mm]	Total Sub. as a % of total Precip	Total Sublimation [mm]	Total Sub. as a % of total Precip	Total Sublimation [mm]	Total Sub. as a % of total Precip
Niwot, CO (Ameriflux)	109	4.8 %	53.3	2.3 %	24.8	1.08 %
Niwot, CO (HRRR)	87.6	5.8 %	46.2	3.1 %	25.2	1.7 %
MW, CO	65.2	3.4 %	22.2	1.17 %	10.5	0.55 %
LSOS, CO	65.6	2.5 %	28.4	1.08 %	34.4	1.31 %
Mt. Hopper, WA	19.8	0.57 %	9.1	0.26 %	8.6	0.25 %

Table 4. The cumulative snow unloading from the canopy as a direct result of the snow unloading parameterizations (i.e., not including loss of snow in the canopy from latent heat fluxes, such as evaporation and sublimation).

Cumulative Canopy Snow Unloading [mm]			
Unloading Parameterization Site	Andreadis et al., (2009)	Hedstrom & Pomeroy, (1998)	Roesch et al., (2001)
Niwot Ridge, CO with Ameriflux	40.4	347	559
Niwot Ridge, CO with HRRR	45.7	282	510
MW, Grand Mesa, CO	20.5	249	489
LSOS, Grand Mesa, CO	50.5	302	504
Mount Hopper, WA	125	364	721

6. Conclusions.

This work demonstrates how time-lapse photography can provide observations of difficult to capture processes and that citizen science observations provide a reliable source of data. While time-lapse photos are a useful tool and provide unique observations, additional data sources are needed in to distinguish between interception schemes.

In a windy environment, such as Niwot Ridge, a tunable wind parameter like the one in Roesch et al., (2001), is useful and yields a higher success than other schemes but does not appear to be transferable to a maritime environment. This parameter is not sensitive to calibration, while an exponential unloading parameter such as the one in Hedstrom & Pomeroy, (1998), is highly sensitive to calibration. If used out of the box, this parameter yields poor results, but once it is calibrated, it provides a reasonable estimate for unloading without including the model physics. In a warm-snow environment such as Mount Hopper, parameterizations that include model physics of snow unloading when there is melt in the canopy, like Andreadis et al., (2009), yields a higher success than the exponential and wind dependent unloading schemes. Andreadis et al. (2009) was developed in a maritime environment and likely captures the physical process impacting unloading at Mount Hopper best.

Large differences were found between the three unloading parameterizations when their impact on the vegetation fluxes are considered. Andreadis et al., (2009) resulted in a larger loss from sublimation at all sites because it retains snow in the canopy the longest between the unloading parameterizations. In a hydrologic model, the difference between unloading from the canopy to the land surface versus sublimation and evaporation determines whether the SWE in the canopy becomes SWE on the ground or if it is returned back to the atmosphere as water vapor. These impacts are even greater when a hydrologic model is coupled to an atmospheric model.

Each of these sites have their own complex physical processes impacting interception and unloading. For instance, MW is a cold and windy site, similar to Niwot Ridge, however, observations show evidence of riming in the canopy which could contribute to snow staying in the tree longer, even with high wind speeds. More work needs to be done to understand the transferability of model parameterizations and the physics of unique snow interception and unloading events. While canopy-snow unloading parameterizations are often overlooked in land surface models, results show that the unloading scheme can have an effect on the duration of

snow in the canopy, impacting the land-surface albedo, and whether canopy-snow contributes to streamflow or is sublimated back to the atmosphere.

Acknowledgements.
We gratefully acknowledge funding support from the Steve and Sylvia Burges Endowed Presidential Fellowship and the NSF Award 1703663, Managing Forests for Snow, Water, and Sustainable Ecosystems. We gratefully acknowledge computational resources from Pangeo and the Computational Hydrology Research Group at the University of Washington.

This publication uses data generated via the *Zooniverse.org* platform, development of which is funded by generous support, including a Global Impact Award from Google, and by a grant from the Alfred P. Sloan Foundation. The data generated from Zooniverse would not be possible without the nearly 7000 individual citizen science volunteers. We are deeply grateful for the thousands of collective hours all the citizen scientists put into generating this data product. Additionally, data used in this research includes 2017 NASA SnowEx time-lapse photography, PhenoCam Network time-lapse images, and OLYMPEX time-lapse images. We would like to thank all the participants from these data missions for their time and are deeply grateful for the availability of these time-lapse images. Funding for AmeriFlux data resources was provided by the U.S. Department of Energy's Office of Science.

This research would not be possible without the tremendous help from collaborators. We thank William Ryan Currier at the National Center for Atmospheric Research, Andrew Bennet and Bart Nijssen of the University of Washington Computational, and all past and current members of the Mountain Hydrology Research Group. The author would also like to give sincere thanks to their advisor, Jessica Lundquist, for her assistance and guidance navigating graduate school and expertise in this research.

Appendix.

Appendix A. Background of Snow Unloading Parameterizations in SUMMA

SUMMA formulates a general set of conservation equations which provides an effortless framework to compare different spatial representations, model parameterizations, and parameter values (Clark et al., 2015a,b,c).

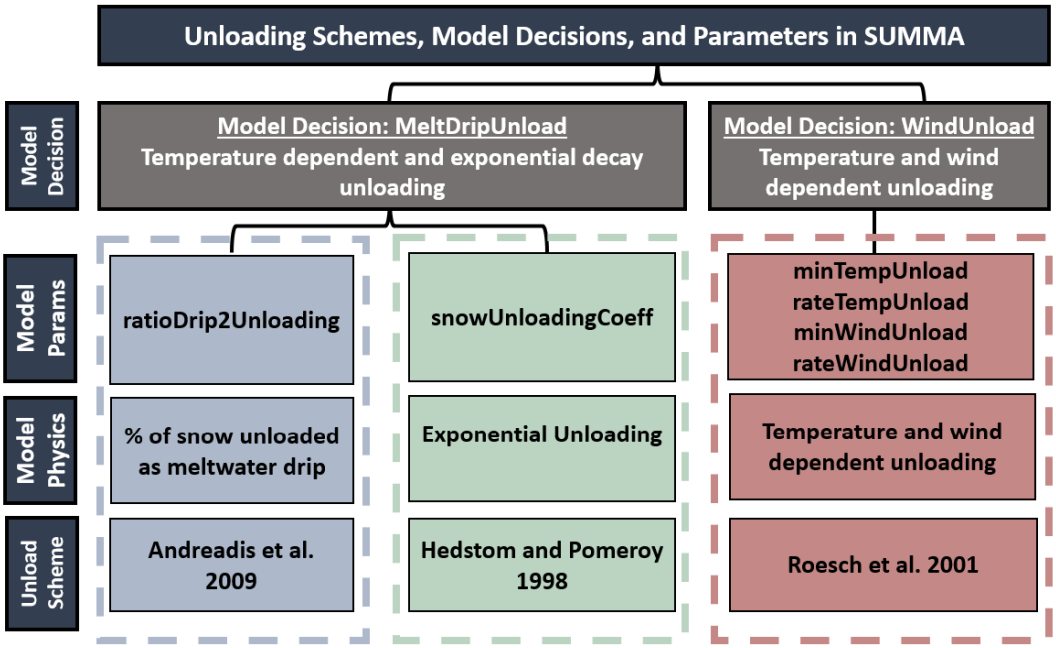

Figure 1. Flowchart for Unloading Parameterizations in SUMMA (version 3.0), where the model decision, model parameters, and model physics are explained with their respective unloading parameterizations from the literature. In blue is (Andreadis et al., 2009), green is (Hedstrom and Pomeroy, 1998) and red is (Roesch et al., 2001).

SUMMA was updated from the original model configuration (Clark et al., 2015) to have a canopy snow unloading model decision, *snowUnload*, with two options: *meltDripUnload* and *windUnload*. The first unloading model decision, *meltDripUnload*, has two independent snow unloading parameterizations built in. One uses an exponential decay function to unload snow from the canopy; the parameter, *snowUnloadingCoeff*, unloads snow from the canopy at a specified exponential rate from the timestep it is intercepted (Hedstrom & Pomeroy, 1998). This unloading parameterization was developed in a cold environments.

The second unloading parameterization within the *meltDripUnload* model decision is a temperature dependent unloading controlled by the model parameter, *ratioDrip2Unloading*, which is a ratio of liquid water drip from the canopy to the snowpack on the ground. (Storck et al., 2002) observed unloading when air temperatures were above 0ºC in warm environments and determined that approximately 40% of the canopy snow is unloaded with meltwater drip.

Snow unloading from the canopy, U, is defined as,

$$U = min(ratioDrip2Unloading \cdot scalarCanopyLiqDrainage),$$

where, the flux of liquid water drainage from the vegetation canopy, kg m^{-2} s^{-1}, *scalarCanopyLiqDrainage,* is defined as,

$$scalarCanopyLiqDrainage = scalarCanopyDrainageCoeff \cdot$$
$$(scalarCanopyLiqTrial - scalarCanopyLiqMax).$$

scalarCanopyLiqTrial is the liquid water accumulating on the vegetation canopy at a given time, kg m^{-2} s^{-1}, *scalarCanopyLiqMax* is the maximum liquid water storage available before canopy drainage begins, kg m^{-2} s^{-1}, and the *scalarCanopyDrainageCoeff* is the tunable canopy drainage coefficient parameter, s^{-1}. (Andreadis et al., 2009) reformulated this parameterization and included it as the snow unloading parameterization in both VIC (Liang et al., 1994) and DHSVM (Wigmosta et al., 1994). The version above exists in SUMMA.

Both (Hedstrom & Pomeroy, 1998) and (Andreadis et al., 2009) unloading parameterizations are including in a single unloading model decision in SUMMA, but can be accessed individually.

The second snow unloading model decision in SUMMA is *windUnload,* which contains both temperature and wind dependent unloading functions formulated by (Roesch et al., 2001) who wanted a better way to represent the albedo over forests. The temperature component of *windUnload* includes a minimum temperature for unloading, controlled by model parameter *minTempUnloadng,* and a rate for temperature dependent unloading, controlled by model parameter *rateTempUnloading.* Similarly, the wind component of *windUnload* includes a minimum wind speed for unloading, controlled by model parameter *minWindUnloading,* and a rate for wind dependent unloading, controlled by model parameter *rateWindUnloading*. The equations for this unloading parameterization are explained further in *Section 3.2.*

Appendix B. SUMMA Model Adaptation: (Roesch et al., 2001) Unloading Parameterization.

As explained in *Section 3.1.*, (Roesch et al., 2001) developed an unloading parameterization using observations from (Betts & Ball, 1997) regarding wind speed and from (Yamazaki et al. 1996) regarding unloading increases with higher winds and air temperatures over 0ºC. This unloading parameterization is used in VISA model (Niu & Yang, 2004), Noah MP model (Niu et al., 2011), and CLASS (Bartlett & Verseghy, 2015).

Now, in SUMMA version 3.0 (Roesch et al., 1997) is including in the *snowUnload* model decision, *windUnload*, which has two dominate unloading equations based off of temperature and wind,

$$windUnload = tempUnloadingFun + windUnloadingFun$$

Where, the *tempUnloadingFun* is defined as,

$$tempUnloadingFun = \frac{scalarCanairTemp - minTempUnloading}{rateTempUnloading}$$

Where the *scalarCanairTemp* is the air temperature within the canopy, the *minTempUnloading* is the minimum temperature required for temperature based unloading to occur, and the

rateTempUnloading is the rate at which snow unloads from the canopy after that minimum temperature is met. Thus, if the air temperature is less than the *minTempUnloading* then this temperature based unloading function is zero.

The second function in this parameterization is the *windUnloadingFun* where, is the wind speed at the top of the canopy, *scalarWindspdCanopyTop*, is greater than or equal to the minimum wind speed required for wind dependent unloading, *minWindUnloading*, then,

$$windUnloadingFun = \frac{scalarWindspdCanopyTop}{rateWindUnloading}$$

where, the *rateWindUnloading* is the rate at which wind is unloading from the canopy once the minimum windspeed is met.

Appendix Table 1. Calibrated and Default model parameter values in SUMMA with suggested ranges from the literature.

Calibrated and Default model parameter values with suggested ranges					
Model Parameter	**Calibrated**	**Default**	**Min**	**Max**	**Literature**
ratioDrip2Unloading [%]	0.4	0.4	0.0	1.0	Andreadis et al., (2009)
snowUnloadingCoeff	1.5E-4	6.4E-4	0.0	1.5E-6	Hedstrom & Pomeroy, (1998)
minTempUnloading [K]	270.15	270.15	260.16	273.16	Roesch et al., (2001)
rateTempUnloading [s^{-1}]	1.87E5	1.87E5	1.0E5	3.0E5	
minWindUnloading [m s^{-1}]	5.0	5.0	0.0	10.0	
rateWindUnloading [s^{-1}]	1.0E5	1.56E5	1.0E5	3.0E5	

References.

Andreadis, K. M., Storck, P., & Lettenmaier, D. P. (2009). Modeling snow accumulation and ablation processes in forested environments. *Water Resources Research*, *45*(5). https://doi.org/10.1029/2008WR007042

Bartlett, P. A., & Verseghy, D. L. (2015). Modified treatment of intercepted snow improves the simulated forest albedo in the Canadian Land Surface Scheme. *Hydrological Processes*, *29*(14), 3208–3226. https://doi.org/10.1002/hyp.10431

Betts, A. K. and Ball, J. H. (1997). Albedo over the boreal forest. *Journal of Geophysical Research.* Vol. 102, No. D24, p. 28,910-28,909. December, 1997.

Bonan, G. B., Pollard, D., & Thompson, S. L. (1992). Effects of boreal forest on global climate. *Nature*, *359*(October), 716–718.

Brodersen, K. H., C. S. Ong., K. E., & Stephan, J. M. Buhmann. (2010). The balanced accuracy and it's posterior distribution. *International Conference on Pattern Recognition.*

Currier, W. R., Thorson, T., & Lundquist, J. D. (2017). Independent Evaluation of Frozen Precipitation from WRF and PRISM in the Olympic Mountains. *Journal of Hydrometeorology*, *18*(10), 2681–2703. https://doi.org/10.1175/jhm-d-17-0026.1

Currier, W. R., Pflug, J., Mazzotti, G., Jonas, T., Deems, J. S., Bormann, K. J., et al. (2019). Comparing Aerial Lidar Observations With Terrestrial Lidar and Snow-Probe Transects From NASA's 2017 SnowEx Campaign. *Water Resources Research*, 1–10. https://doi.org/10.1029/2018WR024533

Essery, R. (1998). Boreal forests and snow in climate models. *Hydrological Processes*, *12*(10–11), 1561–1567. https://doi.org/10.1002/(SICI)1099-1085(199808/09)12:10/11<1561::AID-HYP681>3.0.CO;2-B

Hedstrom, N. R., & Pomeroy, J. W. (1998). Measurements and modelling of snow interception in the boreal forest. *Hydrological Processes*, *12*(10–11), 1611–1625. https://doi.org/10.1002/(SICI)1099-1085(199808/09)12:10/11<1611::AID-HYP684>3.0.CO;2-4

Horel, J., & Blaylock, B. (2019). Archive of the High Resolution Rapid Refresh model. *University of Utah Center for High Performance Computing.* https://doi.org/10.7278/S5JQ0Z5B

Houze, R.A., L.A. McMurdie, W.A. Petersen, M.R. Schwaller, W. Baccus, J.D. Lundquist, C.F. Mass, B. Nijssen, S.A. Rutledge, D.R. Hudak, S. Tanelli, G.G. Mace, M.R. Poellot, D.P. Lettenmaier, J.P. Zagrodnik, A.K. Rowe, J.C. DeHart, L.E. Madaus, and H.C. Barnes, 2017: The Olympic Mountains Experiment (OLYMPEX). *Bull. Amer. Meteor. Soc.*, 98, 2167–2188, https://doi.org/10.1175/BAMS-D-16-0182.1

Klein, A. G., Hall, D. K., and Riggs, G. A. 1998: Improving snow cover mapping in forests through the use of a canopy reflectance model. *Hydrol. Processes*, 12, 1723–1744.

Liang, X., D. P. Lettenmaier, E. F. Wood, and S. J. Burges (1994), A simple hydrologically based model of land surface water and energy fluxes for general circulation models, J. Geophys. Res., 99, 14,415–14,428.

Lundquist, J. D., Dickerson-Lange, S. E., Lutz, J. A., & Cristea, N. C. (2013). Lower forest density enhances snow retention in regions with warmer winters: A global framework developed from plot-scale observations and modeling. *Water Resources Research*, *49*(10), 6356–6370. https://doi.org/10.1002/wrcr.20504

Lundquist, J. D., William Ryan Currier and Bill Baccus. 2018. *GPM Ground Validation Snow Depth Monitoring System OLYMPEX* [indicate subset used]. Dataset available online from the NASA Global Hydrology Resource Center DAAC, Huntsville, Alabama, U.S.A. DOI: http://dx.doi.org/10.5067/GPMGV/OLYMPEX/SNOWTUBE/DATA101

Martin, K. A., J. T. Van Stan II, S. E. Dickerson-Lange, J. A. Lutz, J. W. Berman, R. Gersonde, and J. D. Lundquist, 2013: Development and testing of a snow interceptometer to quantify canopy water storage and interception processes in the rain/snow transition zone of the North Cascades, Washington, USA, *Water Resour. Res.*, 49, doi:10.1002/wrcr.20271

Mass, C. F., and Coauthors, 2003: Regional environmental pre-diction over the Pacific Northwest. *Bull. American Meteorological. Society.*, 84, 1353-1366, doi:10.1175/BAMS-84-10-1353.

Milliman, T., K. and coauthors. 2018. PhenoCam Dataset v1.0: Digital Camera Imagery from the PhenoCam Network, 2000-2015. ORNL DAAC, Oak Ridge, Tennessee, USA. https://doi.org/10.3334/ORNLDAAC/1560

Niu, G. Y., & Yang, Z. L. (2004). Effects of vegetation canopy processes on snow surface energy and mass balances. *Journal of Geophysical Research D: Atmospheres*, *109*(23), 1–15. https://doi.org/10.1029/2004JD004884

Niu, G. Y., Yang, Z. L., Mitchell, K. E., Chen, F., Ek, M. B., Barlage, M., et al. (2011). The community Noah land surface model with multiparameterization options (Noah-MP): 1. Model description and evaluation with local-scale measurements. *Journal of Geophysical Research Atmospheres*, *116*(12), 1–19. https://doi.org/10.1029/2010JD015139

Olson, D. L, and D. Delen. (2008), Advanced Data Mining Techniques, Springer, Berlin Heidelberg.

Roesch, A., Wild, M., Gilgen, H., & Ohmura, A. (2001). A new snow cover fraction parametrization for the ECHAM4 GCM, (December 2000).

Schmidt, R. A and D. R., Gluns 1991: Snowfall interception on branches of three conifer species, *Can. J. For. Res.*, 21, 1262-1269.

Skamarock, W. C., and Coauthors, 2008: A description of the Advanced Research WRF version 3. NCAR Tech. Note NCAR/TN-4751STR, 113 pp., doi:10.5065/D68S4MVH.

Storck, P., Lettenmaier, D. P., & Bolton, S. M. (2002). Measurement of snow interception and canopy effects on snow accumulation and melt in a mountainous maritime climate, Oregon, United States. *Water Resources Research*, *38*(11), 5-1-5–16.

https://doi.org/10.1029/2002wr001281

Thompson, G., P. R. Field, R. M. Rasmussen, and W. D. Hall, 2008: Explicit Forecasts of Winter Precipitation Using an Improved Bulk Microphysics Scheme. Part II: Implementation of a New Snow Parameterization. *Mon. Wea. Rev.*, 136, 5095–5115, https://doi.org/10.1175/2008MWR2387.1.

Wigmosta, M. S., Vail, L. W., Lettenmaier, D. P., Liang, X., Lettenmaier, D. P., Wood, E. F., & Burges, S. J. (1994). A simple hydrologically based model of land surface water and energy fluxes for general circulation models. *Water Resources Research*, *30*(6), 1665–1679. https://doi.org/10.1029/94WR00436